Letters in Applied NanoBioScience
Platinum Open Access Journal (ISSN: 2284-6808)

Article
Volume 9, Issue 3, 2020, 1372 - 1388
https://doi.org/10.33263/LIANBS93.13721388

Chemical Synthesis, Spectral Characterization and Biological Investigations of Novel Triazole-Based Schiff Base Ligand and its Transition Complexes

Honnalagere Mariswamy Vinusha [1], Shiva Prasad Kollur [2,*], Ramith Ramu [3], Prithvi S. Shirahatti [4], Nagendra Prasad M.N. [5], Muneera Begum [1,*]

[1] Department of Chemistry, Sri Jayachamarajendra College of Engineering, JSS Science and Technology University, Mysuru-570 006, India
[2] Department of Sciences, Amrita School of Arts and Sciences, Amrita Vishwa Vidyapeetham, Mysuru Campus, Mysuru, Karnataka – 570 026, India
[3] Department of Biotechnology and Bioinformatics, School of Life Sciences, JSS Academy of Higher Education and Research (JSS AHER), Mysuru - 570 015, India
[4] Post-graduation department of Biotechnology, Teresian College, Siddhartha Nagara, Mysuru - 570 011, India;
[5] Department of Biotechnology, JSS Science and Technology University, JSS Technical Institutional Campus, Mysuru, Karnataka-570006, India
* Correspondence: shivachemist@gmail.com (S.P.K); mbegum20@yahoo.com (M.B);

Scopus Author ID 36237191700

Received: 14.06.2020; Revised: 2.07.2020; Accepted: 3.07.2020; Published: 7.07.2020

Abstract: The present work describes the synthesis and characterization of a Schiff base 5-((3,4-dimethoxybenzylidene)amino)-4*H*-1,2,4-triazole-3-thiol (L) derived from 5-amino-4*H*-1,2, 4-triazole-3-thiol and 3,4-dimethoxy benzaldehyde and its Co(II), Cu(II), Ni(II) and Zn(II) complexes in 2:1 molar ratio (L:M). All the compounds were characterized using mass spectroscopy, 1H NMR, IR spectroscopy, UV-Visible spectroscopy, and TGA. In addition to theses spectral studies, DFT calculations have done. The Schiff base ligand and its complexes were assessed for their *in vitro* antibacterial activity against nine food pathogens, and their potential activity was qualitatively and quantitatively assessed by the presence/absence for the zone of inhibition and MIC values by taking standard antibiotic amoxicillin as positive control and DMSO as a negative control. The free radical scavenging ability of all the samples was assessed by employing a series of *in vitro* assays *viz.*, DPPH, ABTS, and Superoxide, whereas BHA was used as a positive control and results were expressed as EC_{50} values. *In vitro* α-amylase, inhibitory studies revealed that complexes had effective inhibitory potential than the ligand. The synthesized compounds were virtually sketched, and the Docking operation was performed by using the SERFLEXDOCK program as a part of the SYBYL-X 2.1.1 software package (Tripos, USA).

Keywords: Triazole; DFT calculations; Antibacterial studies; Antioxidant studies; Molecular Docking.

1. Introduction

Due to their straightforwardness of synthesis and high yields, Schiff bases have been extensively used as ligands [1-2]. Schiff base ligands containing nitrogen and oxygen donors are exclusive and comprehensive, known for their selectivity and sensitivity towards the metal ions. They exhibit greater properties for many areas, such as important intermediates in organic synthesis, industrial, biological, coordination chemistry, pharmacological, catalytic, and

optical properties [3–6]. A lot of Schiff base complexes with metals have also concerned immense consideration Since of their broad range of biological and medicinal functions, such as antitumor [7], antioxidant, antiviral, antimicrobial, and antineoplastic functions, several of the Schiff base complexes with metals have often become of tremendous concern [8].

Significant attention has also been granted to the synthesis and analysis of Schiff bases and their transition metal complexes. The Schiff base transition metal complexes are not only biologically involved, but they have also been used in many industrial applications such as catalysis of oxidation and polymerization, dyes and pigments, etc.[9-13]. The flexible properties of these compounds have led them to be used in several research areas, including the medicine [14], pharmaceutical [15], electronics [16], dyestuffs [17] and interesting antimicrobial activity [18] studies. Schiff bases, an important class of organic compounds, attract much attention since they are used as models for many biological systems. The biological activity of these compounds is not only dependent on the molecular structure of the compounds. Transition metal complexes of imine ligands are also very precise because the applications of the organic imine ligands have highly developed in coordination with metal ions. The transition metal complexes of the imine ligands are habitually shown more biological activity than the corresponding Schiff bases. The present analysis documents the synthesis accompanied by the characterization of Co(II), Cu(II), Ni(II), and Zn(II) complexes derived from 5-amino-4H-1,2, 4-triazole-3-thiol, and 3,4-dimethoxy benzaldehyde, taking into account the aforementioned details of the Schiff base ligands and their metallic complexes.

2. Materials and Methods

2.1. Materials and methods.

5-amino-4*H*-1,2, 4-triazole-3-thiol, and 3,4-dimethoxy benzaldehyde were purchased from Sigma Aldrich and were used as received. The solvents were purchased from Merck and were dried by standard methods before use. The completion of the reaction was monitored by spotting the reaction mixture on pre-coated silica-gel plates (Merck, India) by thin-layer chromatography (TLC) method, and spots were visualized by UV irradiation. FT-IR spectral measurements were recorded on the Perkin-Elmer spectrometer type 1650 spectrophotometer in the region 4000–400 cm^{-1} using KBr pellets. The ^{1}H NMR and ^{13}C NMR spectra were recorded with a Varian 300 MHz in DMSO-d_6 as a solvent against tetramethylsilane as an internal standard. Mass spectra were recorded on Agilent technology (HP) 5973 mass spectrometer operating at an ionization potential of 70 eV. The electronic absorption spectra were recorded using the UV1800 spectrophotometer (Shimadzu). Thermogravimetric analysis (TGA) was carried out on a Universal TGA Q50 instrument at a heating rate of 2 °C/min between 30 and1000°C.

2.1.1. Antibacterial activity.

To evaluate the antibacterial activity of the ligand and its complexes, the antibacterial agar well diffusion assay was employed [19-20].

2.1.2. Antioxidant assays.

In this study, three standard methods *viz.*, DPPH free radical, ABTS cation radical and superoxide anion radical scavenging activities were determined and measured [21]. Radical

scavenging activities were expressed as EC_{50} values. EC_{50} signifies 50% of free, cation and anion radicals scavenged by the samples tested. The standard antioxidant, Butylated hydroxyl anisole (BHA), was used as a positive control.

2.1.3. Inhibition of α – amylase, and α – glucosidase.

The α-amylase (EC 3.2.1.1, categorized as type-VI B porcine pancreatic α-amylase) inhibition was assayed using soluble starch (1%) as a substrate. The yeast α-glucosidase (EC 3.2.1.20, categorized as type-1 α-glucosidase) inhibition was assayed using the substrate *p*NPG according to the modified method [22].

Acarbose has been used as a positive control. The inhibitory behavior of α-amylase & α-glucosidase was expressed in percentage inhibition and measured with the formulation below

$$\text{inhibition (\%)} = (A_{\text{control}} - A_{\text{sample}}) / A_{\text{control}} \times 100$$

IC_{50} values were determined from a curve relating the % inhibition of each sample to the concentration of the sample. Each experiment was performed in triplicates, along with appropriate blanks. The concentration required to inhibit 50% of the α-glucosidase activity under the specified assay conditions was described as the IC_{50}.

2.1.4. Docking studies.

The synthesized compounds were virtually sketched, and the Docking operation was performed by using the SERFLEXDOCK program as a part of the SYBYL-X 2.1.1 software package (Tripos, USA) and necessary calculations were performed. The overall procedure of the DOCKING program includes ligand preparation, protein preparation, protocol generation, and docking of ligands. Adaptation of Docking protocol and validation of the same was performed by comparing the binding poses of the co-crystallized ligand with amino acids of target protein α-glucosidase (PDB ID: 1G7P) before and after the docking study.

2.1.5. Statistical analyses.

The experiments were performed in triplicates, and the results were expressed as Mean ± SE. Graph pad PRISM software (version 4.03) was used for calculating EC_{50} values and considered statistically significant if the 'p' values were 0.05 or less. Results were subjected to a one-way analysis of variance (ANOVA), followed by Duncan's multiple range test, and the mean comparisons were performed by Duncan's multiple range test using SPSS (version 21.0, Chicago, USA).

2.2. Chemical synthesis.

2.2.1. Synthesis of 5-((3,4-dimethoxybenzylidene)amino)-4H-1,2,4-triazole-3-thiol (L).

Scheme 1 shows the step involved in the synthesis of Schiff base ligand. An equimolar mixture of 5-amino-4*H*-1, 2, 4-triazole-3-thiol, and 3,4-dimethoxy benzaldehyde was taken in a round bottom flask. To this reaction mixture, few drops of glacial acetic acid were added, which acts as a catalyst during the reaction. The reaction mixture was then refluxed at 60-65 °C for 6-8 hours. The precipitate formed was filtered and washed several times with methanol to obtain the final pure product.

Yield: 62%; FT-IR (Nujol, ν/cm^{-1}): 1588 (C=N); 1294 (C-O); 1442 (-OCH_3); 1593 (C=C); 759 (C-S); ^{1}H-NMR (400 MHz, DMSO-d6) δ: 8.61 (N=CH-), 7.12-7.61ppm (Ar-H), Mass (m/z): 264.

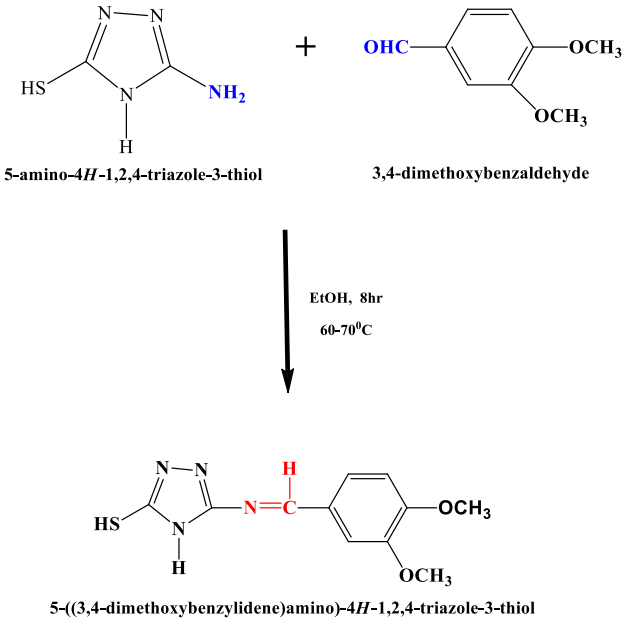

5-amino-4*H*-1,2,4-triazole-3-thiol + 3,4-dimethoxybenzaldehyde

5-((3,4-dimethoxybenzylidene)amino)-4*H*-1,2,4-triazole-3-thiol

Scheme 1. *Synthesis of* 5-((3,4-dimethoxybenzylidene)amino)-4*H*-1,2,4-triazole-3-thiol (L).

2.2.2. Synthesis of complexes (1-4).

2:1 molar ratio of ligand (**L**) and metal salts (Cu, Co, Ni, and Zn) were reacted in order to form the series of metal complexes. The ligand and metal salts were dissolved in methanol separately. To the ethanolic solution of the ligand, metal salt solutions were added dropwise, followed by a few drops of sodium acetate solution to maintain the pH of a solution. After stirring for 4 hours, the precipitate was formed. The obtained precipitate was filtered off, washed with warm ethanol, and dried.

3. Results and Discussion

The Schiff base ligand **(L)** was obtained according to Scheme 1. The proposed structural details were elucidated by FT-IR, ^{1}H NMR, and mass spectral analysis.

3.1. ^{1}H NMR spectroscopy.

In the proton NMR spectrum (Fig. 1), the multiplet signals observed in the region between 7.12-7.61ppm corresponds to aromatic protons, and a singlet observed at 8.61 ppm corresponds to imine proton (CH=N-).

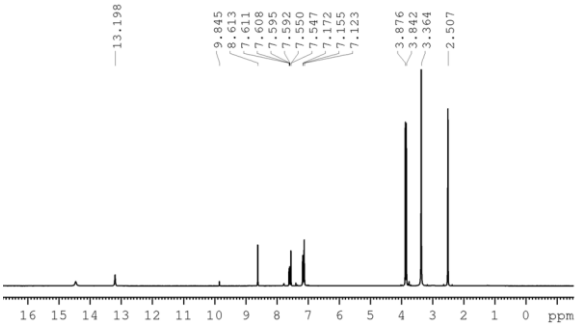

Figure 1. ^{1}H NMR spectrum of ligand **(L).**

3.2. Mass spectrometry.

Further, the mass spectrum of **L** confirmed its formation (Fig. 2). The molecular ion peak was observed at *m/z* =264 consistent with the molecular weight of L and confirm the formation of **L**.

Similarly, the mass spectra of Co(II), Cu(II), Ni(II) and Zn(II) complexes were shown in Fig. S1-S4. In the mass spectrum of complexes, the molecular ion peaks at *m/z* = 585, 590, 585, and 591 affirms the coordination of Co, Cu, Ni, and Zn ions with the ligand, **L**.

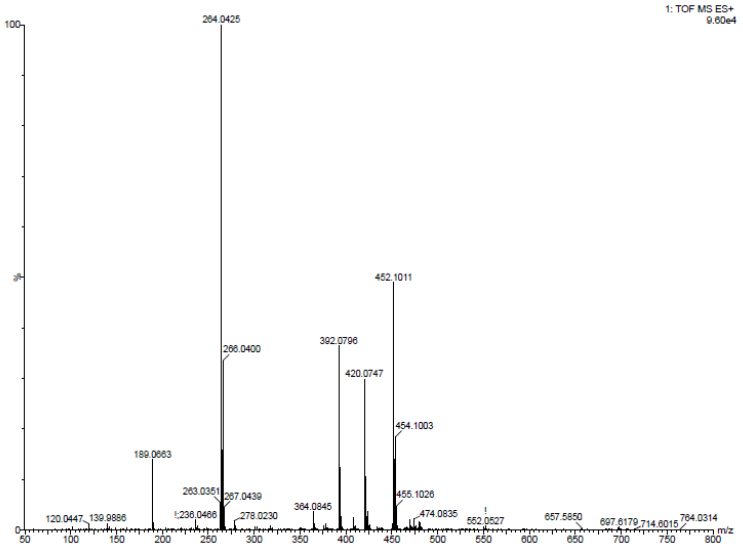

Figure 2. ESI-MS spectrum of 5-((3,4-dimethoxybenzylidene)amino)-4H-1,2,4-triazole-3-thiol **(L).**

3.3. FT- IR spectroscopy.

The presence of C=N group in the ligand was further confirmed by infrared spectral studies. As shown in Fig. 3, a sharp band at 1588 cm^{-1} corresponds to imine group stretching vibration. Similarly, the formation of metal complexes was confirmed by comparing the IR spectra of **L** and their complexes. The FT- IR spectra of all the complexes were shown in Fig. S5 - S8. The IR stretching frequencies of free ligand and its complexes groups have been reported in Table 1. These stretching frequencies support the formation of **L**.

Table 1. IR spectral data of ligand **L** and its complexes in cm^{-1}.

Compounds with formula	**C=N**	**-OCH_3**	**C=C**	**C-S**	**M-N**	**M-S**
$C_{11}H_{12}N_4O_2S$ (L)	1588	1437	1502	756	-	-
L-Cu	1587	1433	1506	746	423	356
L-Co	1596	1439	1509	756	442	361
L-Ni	1579	1433	1503	750	425	355
L-Zn	1580	1420	1484	731	423	342

3.4. UV-visible spectra.

The UV-Visible spectra of ligand and their metal complexes were recorded in DMSO solutions between 200 and 700 nm at room temperature. The UV-Visible spectra of ligand were shown in Fig. 4. In ligand, two bands were observed at 292 and 308 nm, which are attributed to $\pi - \pi^*$ transition of the heterocyclic moieties [23] and $n - \pi^*$ transition of the azomethine group of the ligand, respectively. The UV-Visible spectra of ligand were shown in Fig. S9 – S12. In the metal complexes $\pi - \pi^*$ and $n - \pi^*$ transitions were shifted to longer wavelenghts as a consequences of coordination to metal centre [24]. In Cu(II) complex, the

bands were shifted from 292 to 303 for $\pi - \pi^*$ transition and 308 to 317 nm for $n - \pi^*$ transitions. Similarly, for other metal complexes also $\pi - \pi^*$ and $n - \pi^*$ transitions were shifted to longer wavelengths. This indicates the formation of M-L coordination bond.

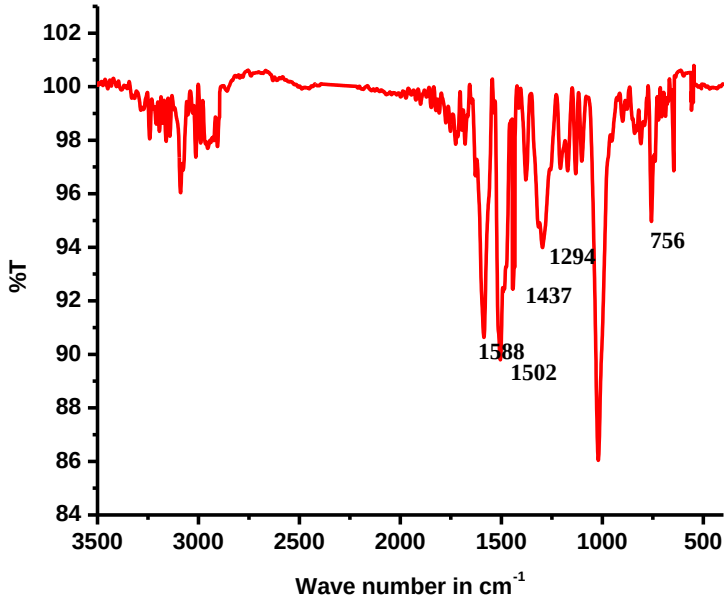

Figure 3. The FT-IR spectrum of ligand **(L).**

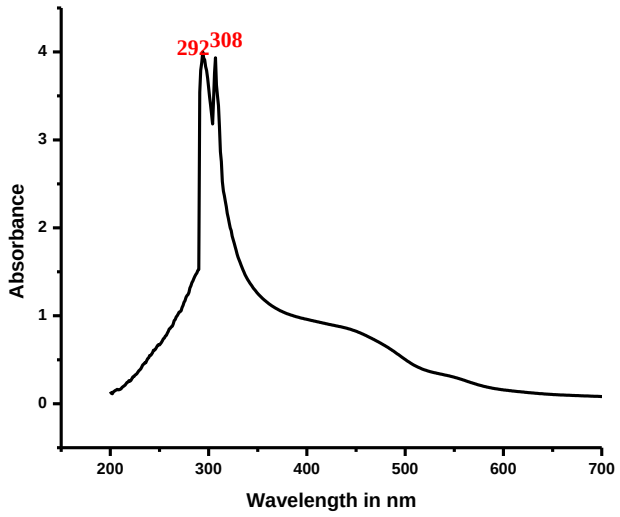

Figure 4. UV-Visible spectrum of ligand **(L).**

3.5. Thermal studies.

In the Zn(II) complex, the decomposition takes place in three steps. In the first step of decomposition up to 220.89°C was probably due to loss of water molecule. The second step begins from 220.89°C to 464.35°C indicates the decomposition of an organic moiety of a molecule. The third decomposition step starts at 464.35°C. It terminates at about 642.47°C, corresponding to the decomposition of **L** (found 43%), leaving behind metal oxide as the end product.

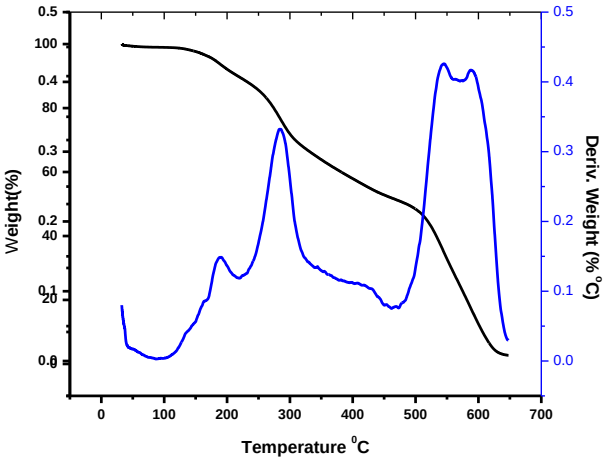

Figure 5. TG and DTA curves of Zn(II) complex.

3.6. Biological activities.

3.6.1. Antibacterial activity.

In the present study, various complexes and ligand were assessed for their *in vitro* antibacterial activity against nine food pathogens and their potential activity were qualitatively and quantitatively assessed by the presence/absence for the zone of inhibition and MIC values. The standard antibiotic amoxicillin was used as a positive control. Impregnated paper discs containing only DMSO used as negative control did not show a zone of inhibition. As shown in Tables 2 and 3, the test samples (ligand & its complexes)exhibited antibacterial activity on different tested strains with variable sensitivity against the six complexes. The Zn(II) complex and the Co(II) complex were found to be sensitive to almost all the tested microorganisms. While the other complexes and the ligand was not active against all the tested microorganisms. Among the complexes tested for antibacterial activity, Zn(II) complex was found to be a potential compound followed by Co(II) complex. On the whole, the MIC values ranged from 3.10 mg/ml up to 4.50 mg/ml(Table 3). All the complexes exhibited higher antibacterial effects than the corresponding ligand. Our results exhibited that all the compounds tested exhibit a broad range of antibacterial activity by inhibiting the growth of foodborne pathogens (Gram-positive and Gram-negative), thereby providing a baseline for future study on potentials of complexes as antibacterial contributors.

3.6.2. Antioxidant activity.

The free radical scavenging ability of test samples was assessed by employing a series of *in vitro* assays *viz.*, DPPH, ABTS, and superoxide, whereas BHA was used as a positive control. Results expressed as EC_{50} values (mg of tests per ml) are summarized in Table 4, revealed that ligand was comparatively lower ($p<0.05$) than complex compounds in radical scavenging activities. In all the assays used in this study, Zn(II) complex and Co(II) complex were ~2.0 – 2.5-fold effective than other complexes, and activities ascended in the order BHA >Zn >Co >Cu>Ni>ligand. In general, Zn(II) complex, followed by Co(II) complex, exhibited a higher free radical scavenging activity in three antioxidant assays. The results revealed that Zn(II) complex possesses strong antioxidant ability and significantly lower ($p<0.05$) than the positive control.

Table 2. Antibacterial activity by disc diffusion for the ligand and its complexes.

		Zone of inhibition* (in "mm")					
		Std.	**Ligand**	**Co**	**Cu**	**Ni**	**Zn**
Gram-positive	*Bacillus cereus*	**12.50 ± 0.19**	**–**	**02.35 ± 0.42**	**–**	**–**	**03.50 ± 0.78**
	Micrococcus luteus	**15.50 ± 0.11**	**03.01 ± 0.35**	**06.60 ± 0.50**	**04.75± 0.45**	**–**	**05.00±1.32**
	Staphylococcus aureus	**18.50 ± 0.19**	**02.90 ± 0.33**	**07.50± 0.47**	**–**	**04.12± 0.68**	**06.05±1.47**
Gram-negative	*Klebsiella pneumoniae*	**11.00 ± 0.74**	**–**	**03.50 ± 1.05**	**–**	**–**	**04.02 ± 0.45**
	Enterobacter aerogenes	**14.00 ± 0.43**	**04.90± 0.50**	**13.06± 0.80**	**05.50±1.25**	**04.00± 0.89**	**16.60± 0.75**
	Escherichia coli	**26.00 ± 0.52**	**04.25 ± 0.50**	**14.90±1.25**	**04.62 ± 0.79**	**06.00±1.47**	**15.50±1.01**
	Pseudomonas fluorescens	**16.50 ± 0.10**	**–**	**04.80±0.54**	**–**	**–**	**05.00± 0.63**
	Pseudomonas aeruginosa	**21.00 ± 0.84**	**–**	**03.10 ± 0.10**	**–**	**–**	**04.50± 0.75**
	Salmonella enteritidis	**09.00 ± 1.03**	**–**	**–**	**–**	**–**	**03.00± 0.65**

** Values are expressed as mean ± SE. (Std.): Amoxicillin; (–): inactive*

Table 3. The minimum inhibitory concentration (MIC) of ligand and its complexes.

		MIC* (in "mg/ml")					
		Std.	**Ligand**	**Co**	**Cu**	**Ni**	**Zn**
Gram-positive	*Bacillus cereus*	**1.50 ± 1.26**	**–**	**NT**	**–**	**–**	**NT**
	Micrococcus luteus	**2.75 ± 0.85**	**NT**	**4.00±1.05**	**NT**	**–**	**03.50±0.52**
	Staphylococcus aureus	**3.25 ± 1.50**	**NT**	**04.50 ±0.59**	**–**	**NT**	**04.10±2.02**
Gram-negative	*Klebsiella pneumoniae*	**4.00 ± 0.51**	**–**	**NT**	**–**	**–**	**NT**
	Enterobacter aerogenes	**2.00 ± 0.48**	**NT**	**3.50±1.24**	**03.75±0.45**	**NT**	**03.10±1.05**
	Escherichia coli	**1.00 ± 0.50**	**NT**	**3.25±0.40**	**NT**	**04.75±0.84**	**03.25±0.45**
	Pseudomonas fluorescens	**3.25 ± 0.95**	**–**	**NT**	**–**	**–**	**04.50± 0.35**
	Pseudomonas aeruginosa	**2.50 ± 0.66**	**–**	**NT**	**–**	**–**	**NT**
	Salmonella enteritidis	**2.00 ± 0.15**	**–**	**–**	**–**	**–**	**NT**

** Values are expressed as mean ± SE. (Std.): Amoxicillin; (–): inactive; (NT): not tested since the ligand and its complexes showed inhibitory effect with inhibition zone ≤05 mm by disc diffusion method.*

Table 4. Antioxidant activity of the ligand and its complexes.

	EC_{50}*,#(mg/ml)		
Test Compounds	Radical scavenging activities		
	DPPH	ABTS	Superoxide
Ligand	15.05 ± 0.78^{f}	20.08±0.20^{e}	18.00±0.55^{e}
Co	06.45 ± 0.84^{c}	05.60±0.30^{b}	04.06±0.16^{b}
Cu	12.08 ± 1.24^{d}	10.02±0.78^{c}	11.34± 0.46^{c}
Ni	13.80 ± 0.24^{e}	12.50± 0.54^{d}	13.54± 0.29^{d}
Zn	05.45 ± 0.60^{b}	05.05 ± 0.15^{b}	3.33±1.27^{b}
Standard ^	0.60 ± 0.10^{a}	0.55 ± 0.35^{a}	0.75 ± 0.45^{a}

** Values are expressed as mean ± SE. Means in the same column with distinct superscripts are significantly different ($p \leq 0.05$) as separated by Duncan's multiple range test.*

 # The EC_{50} value is defined as the effective concentration of the test samples to show 50% of antioxidant activity under assay conditions.

^ Standard: Butylated hydroxyanisole (BHA - positive control).

3.6.3. Inhibitory effects on yeast α-glucosidase and α-amylase.

In vitro α-amylase, inhibitory studies revealed that complexes had effective inhibitory potential than the ligand. The IC_{50} values were found to be 3.25 and 3.75mg/ml for Zn(II) and Co(II), respectively. Acarbose, investigated under the same conditions, had IC_{50} value of 0.50mg/ml. In terms of IC_{50} values, it is evident that diverse complexes tested possessed a strong inhibition of α-amylase and were significantly lower ($p < 0.05$) than acarbose and higher than ligand(Table 5). The inhibition ascended in the order: Acarbose > Zn >Co >Cu>Ni> ligand.

Furthermore, similar studies were performed to assess whether ligand and its complexes also inhibited α-glucosidase, another key carbohydrate hydrolyzing enzyme. The 50% inhibition of α-glucosidase by ligand and its complexes is detailed in Table 5. Results revealed that Zn(II) (IC_{50}: 3.0mg/ml) possessed the highest inhibitory activity followed by Co(II) (IC_{50}: 3.30mg/ml) complex as compared to other complexes, whereas ligand (IC_{50}: 11.20mg/ml) had

the lowest inhibitory effect. The yeast α-glucosidase inhibitory effect (based on IC_{50} values) of ligand & its complexes were comparatively higher ($p < 0.05$) than the therapeutic drug acarbose (IC_{50}:0.50mg/ml).

Table 5. Inhibitory activities of the ligand and its complexes on α-amylase and α-glucosidase enzymes.

Test Compounds	$IC_{50}^{x, y}$ (mg/ml)	
	Enzymes	
	α-amylase	α-glucosidase
Ligand	13.00 ± 0.75^{e}	11.20±0.48^{e}
Co(II) complex	03.75 ± 0.64^{b}	03.30±0.09^{b}
Cu(II) complex	08.06 ± 1.12^{c}	07.08±0.51^{c}
Ni(II) complex	13.45 ± 0.10^{e}	10.00± 2.01 ^{d}
Zn(II) complex	03.25 ± 0.56^{b}	03.00 ± 0.14^{b}
Standard $^{\wedge}$	0.60 ± 0.02^{a}	0.50 ± 0.40^{a}

^{x} *Values are expressed as mean ± SE. Means in the same row with distinct superscripts are significantly different ($p \leq 0.05$) as separated by Duncan's multiple range test.*

^{y} *The IC_{50} value is defined as the inhibitor concentration to inhibit 50% of enzyme activity under assay conditions.*

$^{\wedge}$ *Standard: Acarbose (positive control).*

3.6.4. Molecular docking studies.

A molecular docking study fundamentally defines the binding modes of ligand interaction at the active site of the receptor.

Table 6. Docking scores of compounds with respect to α-glucosidase (PDB ID: 1G7P) enzyme.

Metal complex	Total score	Crash score	Polar score
Co(II) complex	5.16	-1.15	2.03
Zinc(II) complex	5.80	-2.75	1.14

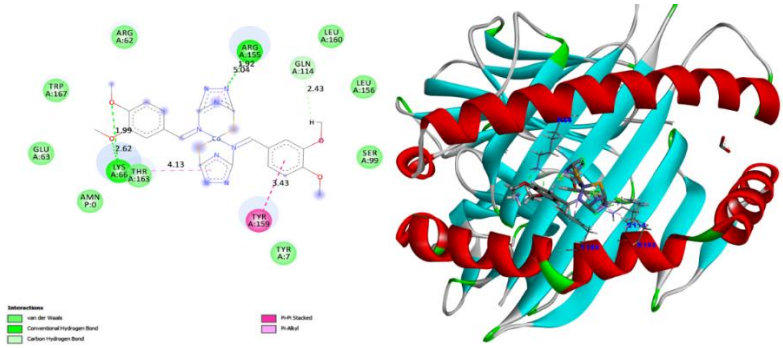

Figure 6. Binding pose of Cobalt with α-glucosidase (PDB ID: 1G7P) enzyme before (2D) and after (3D) Docking studies.

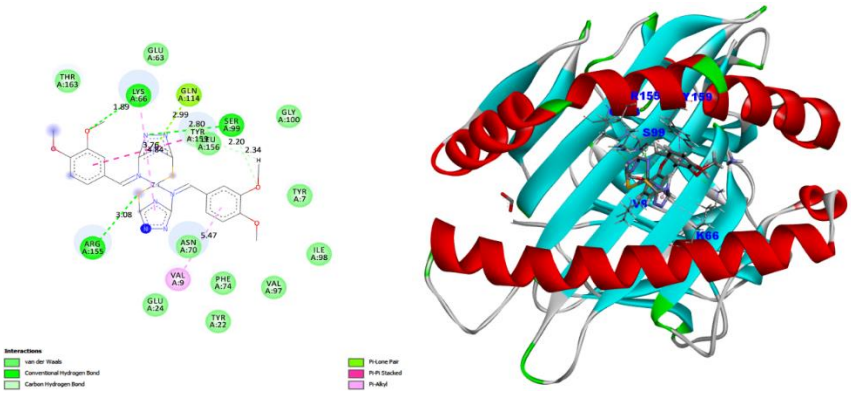

Figure 7. Binding pose of Zinc with α-glucosidase (PDB ID: 1G7P) enzyme before (2D) and after (3D) Docking studies.

In our study, the two compounds with notable α-glucosidase inhibitory activity were subjected to docking studies against α-glucosidase (PDB ID: 1G7P), and the results are shown in Table 6. The inhibition of α-glucosidase (carbohydrate metabolizing enzyme) protein prevents hyperglycemia, and hence it is a striking target for antidiabetic research. The Zn(II) and Co(II) complexes showing α-glucosidase inhibitory activity were subjected to bind the active site of an α-glucosidase protein. The binding interactions with the compounds revealed that almost the two compounds were interacting with threonine, tyrosine, and lysine amino acids (Fig. 4 and 5).

4. Conclusions

To summarize this work, a Schiff base ligand **5**-((3,4-dimethoxybenzylidene)amino)-4*H*-1,2,4-triazole-3-thiol (L) and its Co(II), Cu(II), Ni(II) and Zn(II) complexes were synthesized and characterized using spectroscopic methods. A Schiff base ligand and its all the metal complexes were assayed for antibacterial studies, and the results revealed that among the complexes tested for antibacterial activity, Zn(II) complex was found to be potential compound with the MIC values ranged from 3.10 mg/ml up to 4.50 mg/ml. The free radical scavenging ability of test samples was assessed by employing a series of *in vitro* assays *viz.*, DPPH, ABTS, and superoxide using BHA as a positive control. Results revealed that ligand was comparatively lower ($p<0.05$) than complex compounds in radical scavenging activities. In all the assays used in this study, Zn(II) complex and Co(II) complex were ~2.0 – 2.5-fold effective than other complexes, and activities ascended in the order BHA >Zn >Co >Cu>Ni>ligand. In general, the Zn(II) complex, followed by Co(II) complex, exhibited a higher free radical scavenging activity in three antioxidant assays. *In vitro* α-amylase, inhibitory studies revealed that complexes had effective inhibitory potential than the ligand. The IC_{50} values were found to be 3.25 and 3.75mg/ml for Zn(II) and Co(II), respectively. In terms of IC_{50} values, it is evident that diverse complexes tested possessed a strong inhibition of α-amylase and were significantly lower ($p <0.05$) than acarbose and higher than ligand. The inhibition ascended in the order: Acarbose > Zn >Co >Cu>Ni> ligand. The yeast α-glucosidase inhibitory effect (based on IC_{50} values) of ligand & its complexes were comparatively higher ($p <0.05$) than the therapeutic drug acarbose (IC_{50}:0.50mg/ml). The molecular docking studies reveal that the yeast α-glucosidase inhibitory effect (based on IC_{50} values) of ligand & its complexes were comparatively higher ($p <0.05$) than the therapeutic drug acarbose (IC_{50}:0.50mg/ml).

Funding

This research received no external funding.

Acknowledgments

Authors are thankful to the Head, Department of Polymer Science, SJCE, JSS Science and Technology University, Mysuru for providing characterization facilities. The authors gratefully acknowledge the Director, CFTRI, Mysuru, for providing NMR facility and JSS Science & Technology University, Mysuru, for providing instrumentation facility. KSP thank the Director, Amrita Vishwa Vidyapeetham, Mysuru Campus, Mysuru for infrastructure facilities.

Conflicts of Interest

The authors declare no conflict of interest.

References

1. Tümer, M.; Köksal, H.; Sener, M.K.; Serin, S. Antimicrobial activity studies of the binuclear metal complexes derived from tridentate Schiff base ligands. *Transition Metal Chemistry* **1999**, *24*, 414-420, https://doi.org/10.1023/A:1006973823926.
2. Tümer, M.; Çelik, C.; Köksal, H.; Serin, S. Transition metal complexes of bidentate Schiff base ligands. *Transition Metal Chemistry* **1999**, *24*, 525-532, https://doi.org/10.1023/A:1006982622965.
3. Ekennia, A.C.; Osowole, A.A.; Olasunkanmi, L.O.; Onwudiwe, D.C.; Olubiyi, O.O.; Ebenso, E.E. Synthesis, characterization, DFT calculations and molecular docking studies of metal (II) complexes. *Journal of Molecular Structure* **2017**, *1150*, 279-292, https://doi.org/10.1016/j.molstruc.2017.08.085.
4. Layek, S.; Agrahari, B.; Tarafdar, A.; Kumari, C.; Anuradha; Ganguly, R.; Pathak, D.D. Synthesis, spectroscopic and single crystal X-ray studies on three new mononuclear Ni(II) pincer type complexes: DFT calculations and their antimicrobial activities. *Journal of Molecular Structure* **2017**, *1141*, 428-435, https://doi.org/10.1016/j.molstruc.2017.03.114.
5. El-Sonbati, A.Z.; Diab, M.A.; El-Bindary, A.A.; Abou-Dobara, M.I.; Seyam, H.A. Molecular docking, DNA binding, thermal studies and antimicrobial activities of Schiff base complexes. *Journal of Molecular Liquids* **2016**, *218*, 434-456, https://doi.org/10.1016/j.molliq.2016.02.072.
6. Habibi, M.H.; Shojaee, E.; Ranjbar, M.; Memarian, H.R.; Kanayama, A.; Suzuki, T. Computational and spectroscopic studies of a new Schiff base 3-hydroxy-4-methoxybenzylidene(2-hydroxyphenyl)amine and molecular structure of its corresponding zwitterionic form. *Spectrochimica Acta Part A: Molecular and Biomolecular Spectroscopy* **2013**, *105*, 563-568, https://doi.org/10.1016/j.saa.2012.12.054.
7. Yang, Z.Y.; Yang, R.D.; Li, F.S.; Yu, K.B. Crystal structure and antitumor activity of some rare earth metal complexes with Schiff base. *Polyhedron* **2000**, *19*, 2599-2604, https://doi.org/10.1016/S0277-5387(00)00562-3.
8. Shahid, M.; Salim, M.; Khalid, M.; Tahir, M.N.; Khan, M.U.; Braga, A.A.C. Synthetic, XRD, non-covalent interactions and solvent dependent nonlinear optical studies of Sulfadiazine-Ortho-Vanillin Schiff base: (E)-4-((2-hydroxy-3-methoxy- benzylidene) amino)-N-(pyrimidin-2-yl)benzene-sulfonamide. *Journal of Molecular Structure* **2018**, *1161*, 66-75, https://doi.org/10.1016/j.molstruc.2018.02.043.
9. Berhanu, A.L.; Gaurav; Mohiuddin, I.; Malik, A.K.; Aulakh, J.S.; Kumar, V.; Kim, K.-H. A review of the applications of Schiff bases as optical chemical sensors. *TrAC Trends in Analytical Chemistry* **2019**, *116*, 74-91, https://doi.org/10.1016/j.trac.2019.04.025.
10. Zhang, J.; Xu, L.; Wong, W.-Y. Energy materials based on metal Schiff base complexes. *Coordination Chemistry Reviews* **2018**, *355*, 180-198, https://doi.org/10.1016/j.ccr.2017.08.007.
11. Liu, X.; Manzur, C.; Novoa, N.; Celedón, S.; Carrillo, D.; Hamon, J.-R. Multidentate unsymmetrically-substituted Schiff bases and their metal complexes: Synthesis, functional materials properties, and applications to catalysis. *Coordination Chemistry Reviews* **2018**, *357*, 144-172, https://doi.org/10.1016/j.ccr.2017.11.030.
12. Kaczmarek, M.T.; Zabiszak, M.; Nowak, M.; Jastrzab, R. Lanthanides: Schiff base complexes, applications in cancer diagnosis, therapy, and antibacterial activity. *Coordination Chemistry Reviews* **2018**, *370*, 42-54, https://doi.org/10.1016/j.ccr.2018.05.012.
13. Iscen, A.; Brue, C.R.; Roberts, K.F.; Kim, J.; Schatz, G.C.; Meade, T.J. Inhibition of Amyloid-β Aggregation by Cobalt(III) Schiff Base Complexes: A Computational and Experimental Approach. *Journal of the American Chemical Society* **2019**, *141*, 16685-16695, https://doi.org/10.1021/jacs.9b06388.
14. Hameed, A.; al-Rashida, M.; Uroos, M.; Abid Ali, S.; Khan, K.M. Schiff bases in medicinal chemistry: a patent review (2010-2015). *Expert Opinion on Therapeutic Patents* **2017**, *27*, 63-79, https://doi.org/10.1080/13543776.2017.1252752.
15. Radecka-Paryzek, W.; Pospieszna-Markiewicz, I.; Kubicki, M. Self-assembled two-dimensional salicylaldimine lanthanum(III) nitrate coordination polymer. *Inorganica Chimica Acta* **2007**, *360*, 488-496, https://doi.org/10.1016/j.ica.2006.07.071.
16. Jia, J.H.; Tao, X.M.; Li, Y.J.; Sheng, W.J.; Han, L.; Gao, J.R.; Zheng, Y.F. Synthesis and third-order optical nonlinearities of ferrocenyl Schiff base. *Chemical Physics Letters* **2011**, *514*, 114-118, https://doi.org/10.1016/j.cplett.2011.08.035.
17. Tanaka, K.; Shimoura, R.; Caira, M.R. Synthesis, crystal structures and photochromic properties of novel chiral Schiff base macrocycles. *Tetrahedron Letters* **2010**, *51*, 449-452, https://doi.org/10.1016/j.tetlet.2009.11.062.
18. Jaworska, M.; Wełniak, M.; Zięciak, J.; Kozakiewicz, A.; Wojtczakb, A.J.A. Bidentate Schiff bases derived from (S)-α-methylbenzylamine as chiral ligands in the electronically controlled asymmetric addition of diethylzinc to aldehydes. **2011**, *9*, 189-204, http://dx.doi.org/10.3998/ark.5550190.0012.914.

19. Ramu, R.; Shirahatti, P.; Zameer, F.; Bhadrapura Lakkappa, D.; Prasad M N, N. Evaluation of banana (Musa sp. var. Nanjangud rasa bale) flower and pseudostem extracts on antimicrobial, cytotoxicity and thrombolytic activities. *International Journal of Pharmacy and Pharmaceutical Sciences* **2015**, *7*, 136–140.
20. Vinusha, H.M.; Kollur, S.P.; Revanasiddappa, H.D.; Ramu, R.; Shirahatti, P.S.; Nagendra Prasad, M.N.; Chandrashekar, S.; Begum, M. Preparation, spectral characterization and biological applications of Schiff base ligand and its transition metal complexes. *Results in Chemistry* **2019**, *1*, https://doi.org/10.1016/j.rechem.2019.100012.
21. Razali, N.; Razab, R.; Junit, S.M.; Aziz, A.A. Radical scavenging and reducing properties of extracts of cashew shoots (Anacardium occidentale). *Food Chemistry* **2008**, *111*, 38-44, https://doi.org/10.1016/j.foodchem.2008.03.024.
22. Ramu, R.; Shirahatti, P.S.; Zameer, F.; Ranganatha, L.V.; Nagendra Prasad, M.N. Inhibitory effect of banana (Musa sp. var. Nanjangud rasa bale) flower extract and its constituents Umbelliferone and Lupeol on α-glucosidase, aldose reductase and glycation at multiple stages. *South African Journal of Botany* **2014**, *95*, 54-63, https://doi.org/10.1016/j.sajb.2014.08.001.
23. Beyazit, N.; Çakmak, D.; Demetgül, C. Chromone-based Schiff base metal complexes as catalysts for catechol oxidation: Synthesis, kinetics and electrochemical studies. *Tetrahedron* **2017**, *73*, 2774-2779, https://doi.org/10.1016/j.tet.2017.03.081.
24. Frau, J.; Flores-Holguín, N.; Glossman-Mitnik, D. Chemical Reactivity Properties, pK(a) Values, AGEs Inhibitor Abilities and Bioactivity Scores of the Mirabamides A–H Peptides of Marine Origin Studied by Means of Conceptual DFT. *Mar Drugs* **2018**, *16*, 302–19, https://doi.org/10.3390/md16090302.

Supplementary files

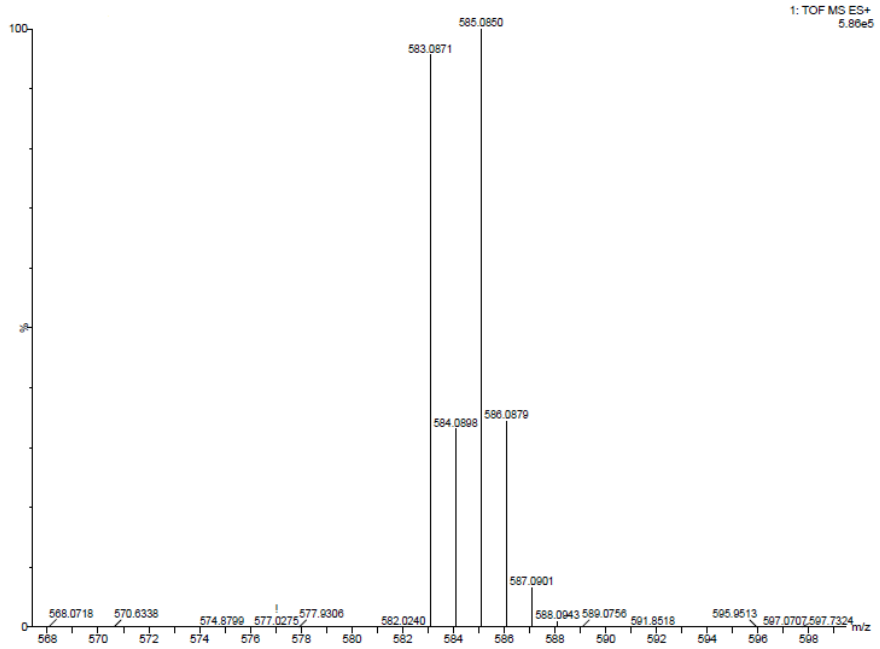

Figure S1: Mass spectrum of **Co(II)** complex.

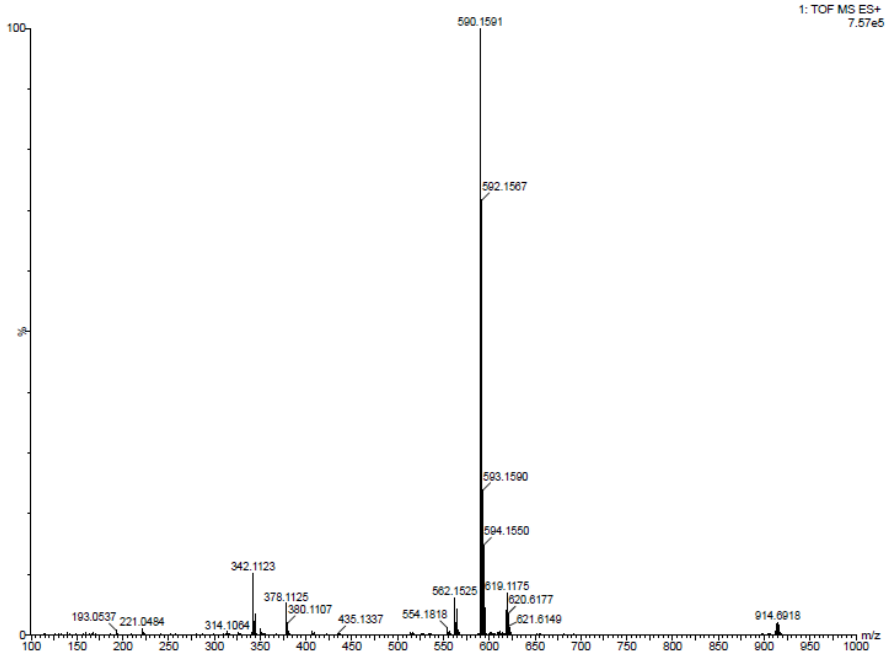

Figure S2. Mass spectrum of **Cu(II)** complex.

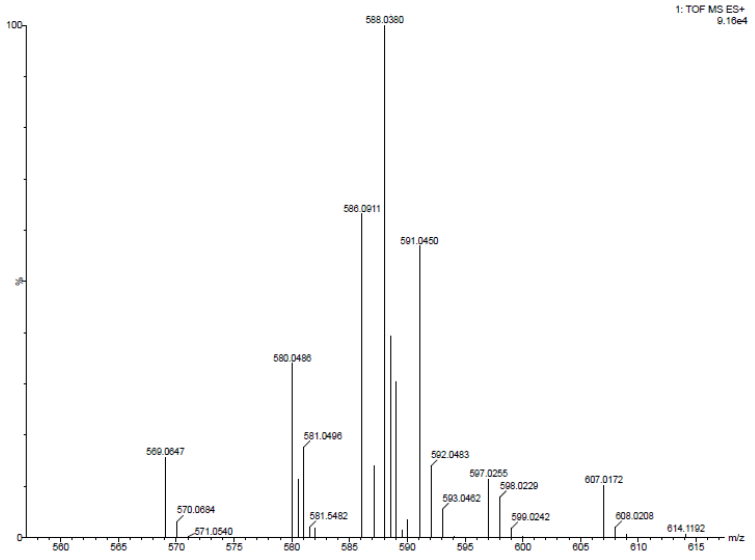

Figure S3. Mass spectrum of **Ni(II)** complex.

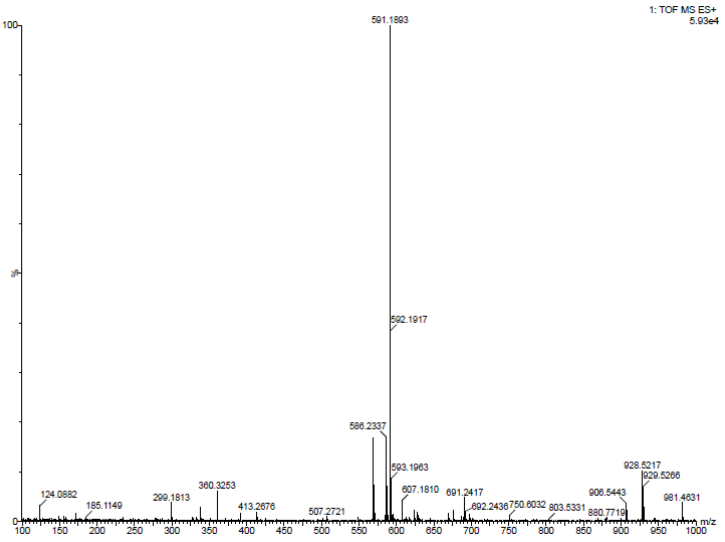

Figure S4. Mass spectrum of **Zn(II)** complex.

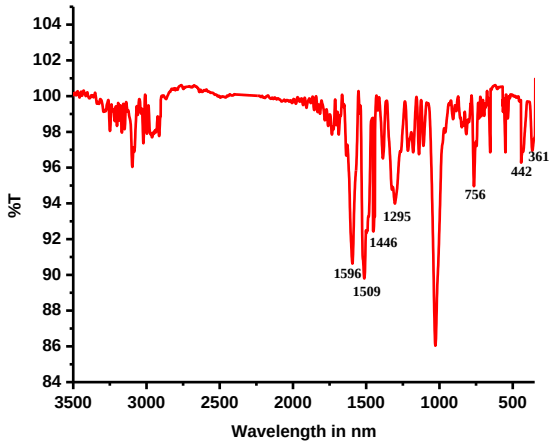

Figure S5. FT-IR spectrum of**Co(II)** complex.

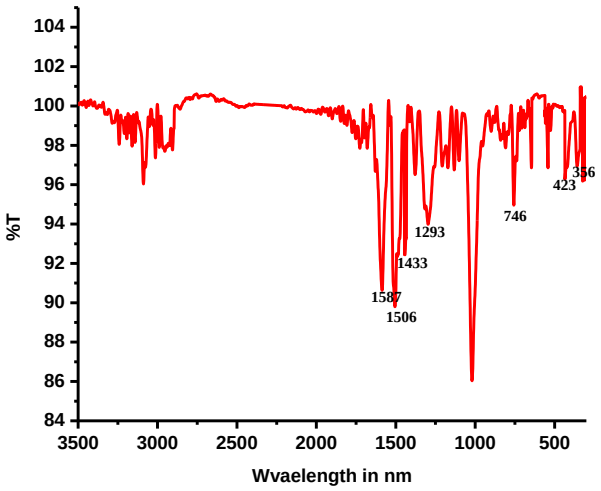

Figure S6. FT-IR spectrum of **Cu(II)** complex.

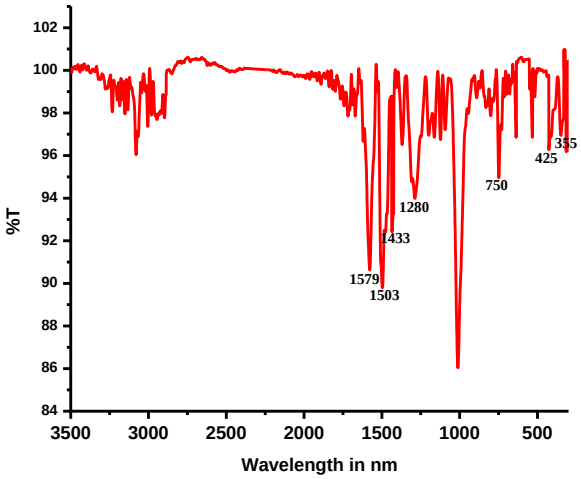

Figure S7. FT-IR spectrum of **Ni(II)** complex.

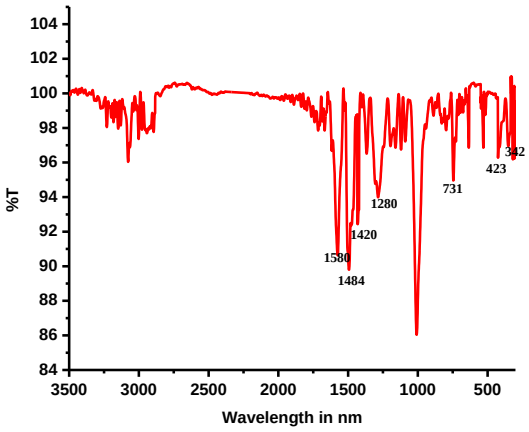

Figure S8. FT-IR spectrum of **Zn(II)** complex.

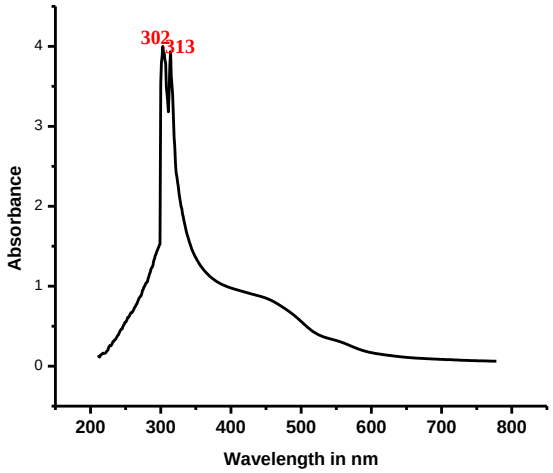

Figure S9. UV-Visible spectrum of **Co(II)** complex.

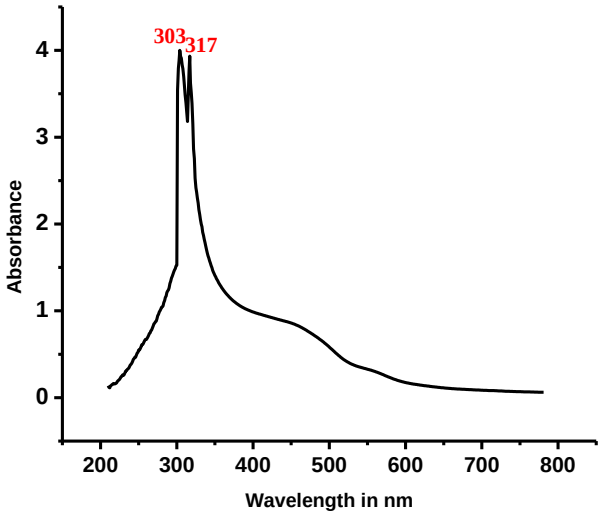

Figure S10. UV-Visible spectrum of **Cu(II)** complex.

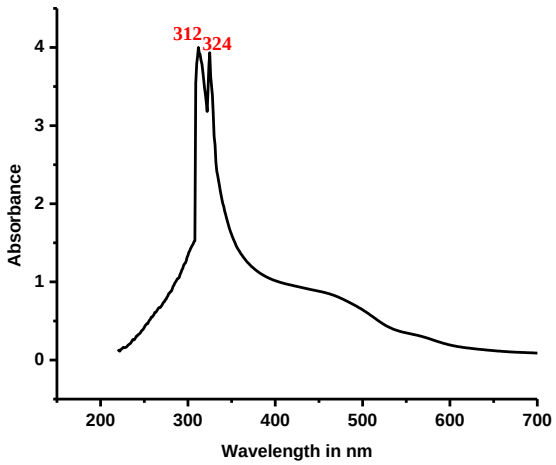

Figure S11. UV-Visible spectrum of **Ni(II)** complex.

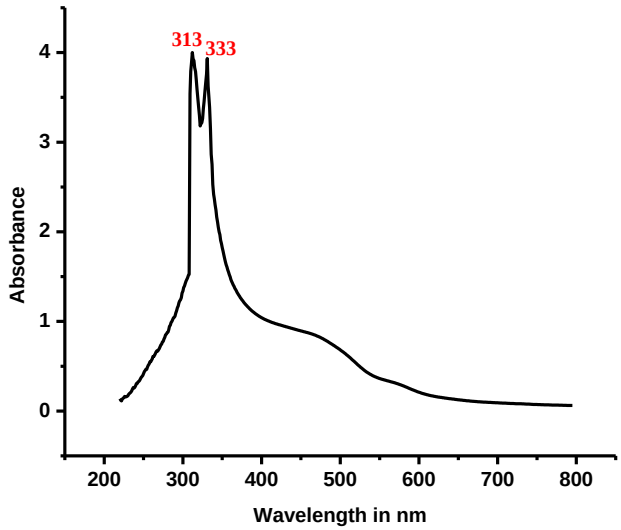

Figure S12. UV-Visible spectrum of **Zn(II)** complex.